Development of a Spin-Light Polarimeter for the EIC

December 12, 2013

Dipangkar Dutta (PI), James Dunne, Edward Leggett, Prajwal Mohanmurthy, Mitra Shabestari
Mississippi State University, Mississippi State, MS
Wouter Deconinck (Co-PI), Valerie Gray
College of William and Mary, Williamsburg, VA
Abhay Deshpande (Co-PI)
Stony Brook University, Stony Brook, NY
Frank Maas (Co-PI)
Johannes Gutenberg-Universität, Mainz, Germany
Kent Paschke (co-PI)
University of Virginia, Charlottesville, VA
Paul Reimer (Co-PI)
Argonne National Lab, Argonne, IL
Dave Gaskell (Co-PI)
Thomas Jefferson National Accelerator Facility, Newport News, VA

Progress Report

Reporting Period: From: 06/2013 to 12/2013

We have completed the Geant4 study of the prototype spin-light polarimeter. The simulation was used to study several systematic uncertainties, such as the effect of background radiation, the position/alignment of the collimators and the alignment of the ion chambers, on the asymmetry signal. The results of these studies have been tabulated in the systematic uncertainties table in the updated proposal below. These results were reported at the recent INPC conference in Florence, Italy and the PSTP conference in Charlottesville, Virginia. An article detailing the conceptual design has been accepted for publication in IEEE Transactions in Nuclear Science [1].

We have carefully estimated the Synchrotron radiation (SR) load on the slits and collimators and we have discussed these results below and in the proposal. We have also been consulting with Vadim Ptitsyn from BNL about handling the expected SR load. The total SR power incident on the slits and collimators will increase as the fourth power of the electron beam energy, and will increases linearly with beam current. The SR power load for a 100 μA beam current and B_{wigg} = 4 Tesla wiggler is shown in Fig. 1. Although the total SR power is small compared to the SR power loads ($\sim$ MW) that is expected at eRHIC, it is the power density in W/mm^2 that determines the figure of merit [2]. In the spin-light polarimeter the SR power will be distributed over an area of $\sim$ 100 mm $\times$ 1 mm. Materials such as GlidCop (Al and Al_20_3 dispersion strengthened copper) [3] and configurations such as crotch absorbers [4] have been demonstrated to withstand power densities of $\sim$ 100 W/mm^2. These factors impose practical limitations on the highest electron beam energies and the highest currents below which a spin-light polarimeter would be feasible. We estimate that it is best suited for the 4 - 20 GeV energy range for currents less than $\sim$ 10 mA.

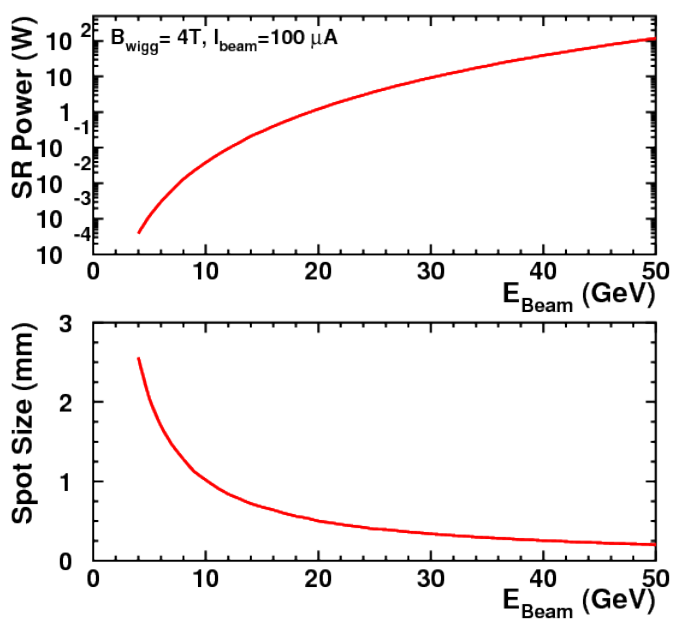

Figure 1: (top) The total SR power radiated as a function of the electron beam energy, for a 100 μA beam current and B_{wigg} = 4 Tesla. (bottom) The vertical size of the SR beam spot as a function of the electron beam energy, at a distance of 10 m from the wiggler magnet.

It has been suggested that due to the coupling between the beam polarization and luminosity, it may be necessary to monitor both the beam polarization and the polarization bunch-current correlation of the beam. Although, a bunch-by-bunch measurement of the polarization is desirable, it is not feasible for any of the energy recovery linac based designs of the electron accelerator. A bunch-by-bunch measurement is feasible only in a ring based design of the electron accelerator where there are multiple collisions between the different bunches. Moreover, for the proposed eRHIC "Gatling" electron gun design, there are expected inter-cathode fluctuations in polarizations. We have learned from the machine experts that the electron gun cathode will have an electronic tagging pulse/signal (similar to the signal used to tag the beginning of a helicity reversal), thus one can use this electronic tag as a means to accumulate counts from a particular cathode. Thus, it will be possible to measure the relative beam polarization of individual cathodes and monitor the inter-cathode variation in polarization.

A spin-light polarimeter would average over most electron source characteristics. The device would be an integrating polarimeter, that would provide the polarization of the electron beam averaged over 5 - 15 second periods. The aim of such a polarimeter is to provide an independent non-invasive high precision relative measurement of the beam polarization as a cross check and as a means of reducing systematic uncertainties. Absolute polarization can be measured only at the few % level. However, it is the only devices which will allow the simultaneous monitoring of the longitudinal as well as the transverse polarization.

In view of the successful simulation we are resubmitting our proposal below. The aim of the proposal is to develop a split-plane differential ionization chamber required for a spin-light polarimeter and to demonstrate the feasibility of such a polarimeter by measuring the spatial asymmetry of the synchrotron radiation from longitudinally polarized multi-GeV electrons.

The Proposal

1 Executive Summary

We have assembled an international collaboration of electron polarimeter experts for research and development towards a new type of polarimeter called a spin-light polarimeter that would be capable of measuring the electron beam polarization at the EIC. A spin-light polarimeter requires a position sensitive hard X-ray detector. We propose to develop a split-plane differential ionization chambers as a position sensitive X-ray detectors. The differential ionization chambers will be initially tested at an X-ray source such as the Advanced Photon Source (APS) at Argonne national Lab (ANL), and then it will be tested using a multi-GeV polarized electron beam and the chicane magnets of the Compton polarimeters at JLab or an equivalent set of existing bending magnets at other electron accelerators. This would be the first demonstration of the spin-light from a longitudinally polarized electron.

2 Introduction

Polarized electrons and ion beams are an essential part of the EIC program to address fundamental questions in QCD, such as how gluons contribute to the spin structure of the nucleon. The EIC also has a unique ability to measure parity-violating structure functions involving $W^{\pm}$ and Z boson mediated interactions. The EIC will enable precision tests of the Bjorken sum rule, a fundamental test of QCD, and thereby allow precision measurements of the strong coupling constant, α_s. It would also allow measurements of generalized parton distributions (GPD) and transverse momentum distributions (TMD), which would lead to 3-D mapping of the proton's internal structure. The high energy and luminosity combined with polarized electrons and protons as well as a variety of heavy ion targets will provide a wealth of data in a regime never explored before.

The parity-violating, right-left, deep-inelastic polarized *ep* and *ed* asymmetries can be used to precisely determine the running of $\sin^2\theta_W(Q)$ as a function of Q^2. The comparison of those measurements with precision values obtained from other lower energy or Z-pole studies can be used to find hints of "new physics". Alternatively, the overall world average of $\sin^2\theta_W$ can be compared with precisely determined quantities such as α_{EM}, G_F, m_Z, and m_W to test the SM at the quantum loop level and probe "new physics" effects. The projected uncertainties of past, present and future EIC measurements of $\sin^2\theta_W$ are shown in Figure 2 [5][1].

This entire program, especially the parity-violating electroweak program at the EIC, will place stringent requirements on the precision polarimetry of the electrons. The determination of the polarization of the electron beam is one of the dominant systematic uncertainties for this program. In order to achieve the desired high precision, the polarization of the electron beam must be monitored continuously with a systematic uncertainty of <1%. In addition to being precise, the polarimeters must be non-invasive and must achieve the desired statistical precision in the shortest time possible. These ambitious goals can only be achieved if multiple independent and high precision polarimeters are used simultaneously. In addition to being precise, the polarimeters must be non-invasive and must achieve the desired statistical precision in the shortest time possible. Compton and Møller polarimeters are typically the polarimeters of choice for these experiments and are essential to achieve the desired precision. However, a complimentary polarimetry technique based on the spin dependence of synchrotron radiation, referred to as "spin-light," can be used as a relative polarimeter. A spin-light polarimeter could provide additional means for improving the systematic uncertainties

[1] We thank Yingchuan Li for an updated version of this figure.

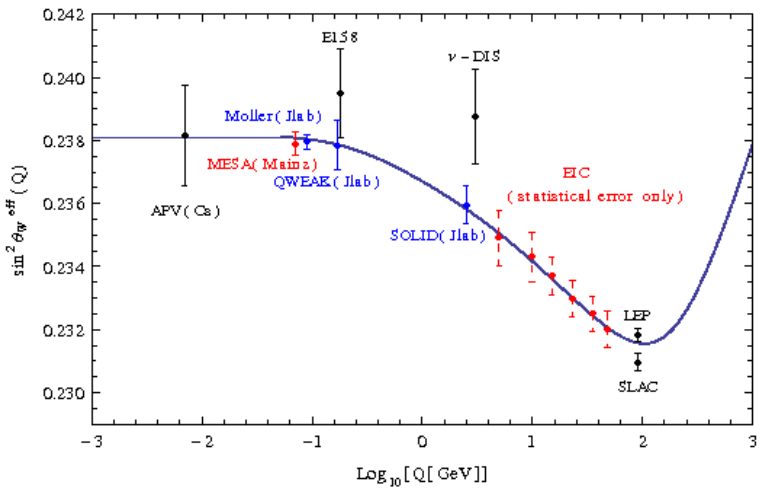

Figure 2: The projected uncertainties of past, present and future EIC measurements of $\sin^2\theta_W$.[5]

and when calibrated against a Compton/Møller polarimeter it could provide a stable continuous monitoring of the beam polarization.

We propose to develop a novel continuous non-invasive polarimeter based on the spin dependence of synchrotron radiation (SR), referred to as "spin-light". The proposed spin-light polarimeter can achieve 1% statistical precision in measurement cycles of less than few minutes for 4 - 20 GeV electron beams with beam currents of < 10 mA. The proposed polarimeter would facilitate cross-checks and systematic studies. The redundancy, both in the measurement and continuous monitoring of the beam polarization, will provide a new benchmark in precision electron beam polarimetry. We present a description and a conceptual design of a spin-light polarimeter, and propose a R&D program to develop the detector technology which is essential for the success of a spin-light polarimeter.

Møller and Compton polarimeters have a proven track record of very high precision, the JLab Hall-C Møller polarimeter has an instrumental uncertainty of 0.47% [6] and absolute uncertainty of 0.85% [7], while the Compton polarimeter used in the SLD experiment achieved an instrumental uncertainty of 0.4% [8] and an absolute uncertainty of 0.5% [8], hence they are essential for any PVES program. However, a spin-light polarimeter would have a few operational and instrumental advantages over conventional polarimeters, such that when used in parallel with Compton/Møller polarimeters they might help reduce the systematic uncertainties and achieve the very high precision essential for the future PVES program. For example, Møller polarimeters use a polarized Fe target, and the polarization of the target is difficult to determine and may depend on the beam intensity. Moreover, Møller polarimeters operate at low current, and are invasive to the primary experiment. Compton polarimeters require a stable laser (the photon target) and are very sensitive to backgrounds. The proposed spin-light polarimeter is a target free device, hence it should be easier to operate over long periods, with its stability governed just by the stability of the electron beam. Moreover, this novel polarimeter would facilitate cross-checks and systematic studies when used with other conventional polarimeters. On the other hand, one of the disadvantages is that the proposed device can achieve comparable instrumental uncertainties only as a relative polarimeter, whereas the absolute polarization is what is required in the PVES experiments. Nevertheless a precise and stable relative polarimeter can be a very useful device. The spin-light polarimeter could be used in conjunction with a Compton polarimeter, such that the difficult to operate Compton polarimeter is used for calibration and the easier to operate and stable spin-light polarimeter is

Table 1: A comparison of the Compton, Møller and Spin-light polarimeters. The systematic uncertainties for the Spin-light polarimeter are described in Sec. 5.5.

Compton	Spin-Light	Møller
non-invasive, continuous	non-invasive, continuous	invasive
analyzing power energy dependent	analyzing power energy dependent	analyzing power energy independent
high currents	moderately high currents	low currents
target is 100% polarized (requires stable laser)	no target needed	target is $< 10\%$ polarized
electron & photon detection are two independent measurements	beam left & right detectors provide two independent measurements	no independent measurements possible
high precision absolute polarimeter	high precision relative polarimeter	high precision absolute polarimeter
Best reported [8] instrumental uncertainty: 0.4%	expected instrumental uncertainty: 0.6%	Best reported [6] instrumental uncertainty: 0.47%
Best reported [8] absolute uncertainty: 0.5%	estimated absolute uncertainty: $\sim$2.5%	Best achieved [7] absolute uncertainty: 0.85%

used to continuous monitor the beam polarization. Moreover, only the Møller and the spin-light polarimeters allow measurement of the transverse component of a longitudinally polarized electron beam in the same device. The key features of conventional polarimeters and a spin-light polarimeter are summarized in Table 1.

3 Quantum Theory of Synchrotron Radiation

The exact expression for SR intensity including quantum corrections was calculated by Sokolov, Ternov and Klepikov, based on the solution to the Dirac equation in the framework of quantum electrodynamics [16]. They showed that at energies above a few 100 MeV, there would be fluctuations in the radius of the electron orbit leading to radial oscillations [17] of the electron trajectory and quantum widening of the trajectory similar to Brownian motion. These oscillations and widening of the trajectory are essential in determining the dynamics of electrons in an accelerator, specially storage rings. Sokolov and Ternov also developed the mathematics required to describe the spin of relativistic electrons moving in an external electromagnetic field [18, 19], which allowed them to calculate the electron spin related properties of SR.

The power radiated by electrons undergoing transitions $n \rightarrow n^{'}$ (related to the radius of the electron orbit), $s \rightarrow s^{'}$ (quadratic fluctuation of the radius) and $j \rightarrow j^{'}$ (spin orientations with respect to the magnetic field), integrated over angles and summed over polarization states, is given by [18, 19]:

$$P = P^{clas} \times \frac{9\sqrt{3}}{16\pi} \sum_{s^{'}} \int_0^\infty \frac{ydy}{(1+\xi y)^4} I^2_{ss'}(x) F(y), \tag{1}$$

where,

$$\begin{aligned} F(y) &= \frac{1+jj^{'}}{2}[2(1+\xi y)\int_y^\infty K_{5/3}(x)dx \\ &+ \frac{1}{2}\xi^2 y^2 K_{2/3}(y) - j(2+\xi y)\xi y K_{1/3}(y)] \\ &+ \frac{1-jj^{'}}{2}\xi^2 y^2 \left[K_{2/3}(y) + lK_{1/3}(y)\right] \end{aligned} \tag{2}$$

where P^{clas} is the classical expression for SR power radiated, $y = \frac{\omega}{\omega_c}$, $x = \frac{3}{4}\frac{\xi\gamma^3 y^2}{(1+\xi y)^2}$, $I_{ss'}$ are the Laguerre functions, $K_n(x)$ are modified Bessel functions, and $\xi = \frac{3}{2}\frac{B}{B_{crit}}\gamma$ is the critical parameter. Because, $B_{crit} = 4.41\times\ 10^9$ Tesla we have $\xi << 1$ for magnetic fields used at all man-made accelerators and the above expression can be expanded in terms of the critical parameter ξ to get [20];

$$\begin{aligned} P &= P^{clas}[(1 - \frac{55\sqrt{3}}{24}\xi + \frac{64}{3}\xi^2) \\ &- (\frac{1+jj^{'}}{2})(j\xi + \frac{5}{9}\xi^2 \frac{245\sqrt{3}}{48} j\xi^2) \\ &+ (\frac{1-jj^{'}}{2})(\frac{4}{3}\xi^2 + \frac{315\sqrt{3}}{432} j\xi^2) + ...] \end{aligned} \tag{3}$$

These quantum corrections to the classical expression for charge radiation (P^{clas}) involve contributions from the electron recoil effects of radiation, interference of the charge radiation and radiation due to the intrinsic magnetic moment of the electron, magnetic moment radiation due to Larmor

precession, magnetic moment radiation due to Thomas precession, interference between the Larmor and Thomas radiation and radiation due to the anomalous magnetic moment of an electron [20]. The lowest order spin-dependent correction is of order ξ and the lowest order spin-flip correction term is of order ξ^2. The difference (of order ξ) between the expression for power radiated by polarized and unpolarized (spin averaged) electron beams has the form,

$$P^{pol} - P^{unpol} = -j\xi P^{clas} \int_0^\infty \frac{9\sqrt{3}}{8\pi} y^2 K_{1/3}(y) dy. \tag{4}$$

The above expression is directly related to the spin polarization of an electron beam j, hence the difference $P^{pol} - P^{unpol} = P^{spin}$ can be called "spin-light" [18, 19]. This offers a new possibility for visual or direct observation of the polarization characteristics of an electron beam by determining the SR power at a fixed range of spectral frequency.

The spin dependence of the SR was verified at the VEPP-4 storage ring in Novosibirsk [21], using a 3 pole wiggler magnet (called a magnetic snake). The intensity of the SR produced by the wiggler for transversely polarized electrons was monitored while the beam was periodically depolarized using a RF field. The measured variation in SR intensity with polarization matched exactly with the expectation from the Sokolov-Ternov theory. This spin dependent part of the SR has been successfully used at the VEPP-4 to monitor the transverse polarization of the electron beam.

The spin-flip term has a unique effect on circular accelerators. The radiation probability with spin flip is given by $w^{\uparrow\downarrow} = \frac{1}{\tau}\left(1 + j\frac{8\sqrt{3}}{15}\right)$, where $j = 1$ is for spin along the magnetic field and $j =$ -1 is for spin opposite to the magnetic field [18]. Using this relation, Sokolov and Ternov had predicted that, over time the beam in a circular accelerator would eventually become polarized opposite to the direction of the magnetic field. In other words the beam of a circular accelerator becomes transversely polarized over time via self polarization. This phenomena known as the Sokolov-Ternov self polarization was first observed at the French storage ring [22] at Orsay and is now routinely used to polarize beams at circular electron accelerators such as DESY.

4 Spin Light

In the discussion above the spin orientation j is relative to the magnetic field that produces the SR, with $j = 1$ along the magnetic field. Polarized electron beams have longitudinal (p_z), transverse horizontal (p_x) and transverse vertical (p_y) components relative to the beam direction. For a vertically oriented magnetic field, the total SR power from transverse horizontally (vertically) polarized electrons, ignoring spin flip terms and other terms of order ξ^2, is given by [18]:

$$\begin{aligned} P_\gamma(tran) &= \frac{9n_e}{16\pi^3}\frac{ce^2}{R^2}\gamma^5 \int_0^\infty \frac{y^2 dy}{(1+\xi y)^4} \oint d\Omega (1+\alpha^2)^2 \\ &\times \quad [K_{2/3}^2(z) + \frac{\alpha^2}{1+\alpha^2} K_{1/3}^2(z) \\ &-(+) \quad p_{x(y)} \xi y \frac{1}{\sqrt{1+\alpha^2}} K_{1/3}(z) K_{2/3}(z)], \end{aligned} \tag{5}$$

where n_e is the number of electrons, $z = \frac{\omega}{2\omega_c}(1+\alpha^2)^{3/2}$, and $\alpha = \gamma\psi$, where ψ is the vertical angle in the frame of the moving electron. The rest of the symbols are as defined in previous instances. The polarization dependent term in the above expression is an even function of the vertical angle therefore when integrated over all angles it makes the total SR power spin dependent. Thus by

measuring this spin dependence in the total SR power radiated one can measure the transverse polarization of the electron beam. As mentioned earlier this phenomena was demonstrated at the VEPP-4 storage ring in Novosibirsk [21].

On the other hand, the total SR power from longitudinally polarized electrons, ignoring spin flip terms and other terms of order ξ^2, is given by [18]:

$$\begin{aligned} P_\gamma(long) &= \frac{9n_e}{16\pi^3}\frac{ce^2}{R^2}\gamma^5\int_0^\infty \frac{y^2dy}{(1+\xi y)^4}\oint d\Omega(1+\alpha^2)^2 \\ &\times [K_{2/3}^2(z)+\frac{\alpha^2}{1+\alpha^2}K_{1/3}^2(z) \\ &+ p_z\xi y\frac{\alpha}{\sqrt{1+\alpha^2}}K_{1/3}(z)K_{2/3}(z)], \end{aligned} \tag{6}$$

The spin dependent term in the above expression is an odd function of the vertical angle therefore when integrated over all angles it goes to zero and the total SR power for longitudinally polarized electrons is spin independent. However, the power radiated into the space above ($0 < \psi < \pi/2$) and below ($-\pi/2 < \psi < 0$) the orbital plane of the electron are different and the difference between them is spin dependent. Therefore, by measuring this spatial asymmetry one can monitor the longitudinal polarization of the electron beam. For $\xi y << 1$, if we divide the above expression by the energy of the radiated photon, $E_\gamma = \frac{3}{2}\frac{\hbar c}{R}\gamma^3 y$ we get the total number of photons radiated into a finite horizontal angle $\Delta\theta$ as,

$$\begin{aligned} N_\gamma &= \frac{3}{4\pi^2}\frac{1}{137}\frac{I_e}{e}\gamma\Delta\theta\int_{y_1}^{y_2} ydy\int_{-\alpha}^{\alpha}(1+\alpha^2)^{3/2} \\ &\times \left[K_{2/3}^2(z)+\frac{\alpha^2}{1+\alpha^2}K_{1/3}^2(z)\right]d\alpha, \end{aligned} \tag{7}$$

where I_e is the beam current. The difference in the photon flux radiated in the the space above and below the electron orbit is given by,

$$\begin{aligned} \Delta N_\gamma(p_z) &= \frac{3}{\pi^2}\frac{1}{137}\frac{I_e}{e}p_z\xi\gamma\Delta\theta\int_{y_1}^{y_2} y^2dy\int_0^{\alpha}\alpha(1+\alpha^2)^{3/2} \\ &\times K_{1/3}(z)K_{2/3}(z)d\alpha \end{aligned} \tag{8}$$

To examine the size and characteristics of the spin dependence we have numerically integrated the above two expressions for longitudinally polarized electron with 100% polarization, in a 4 Tesla magnetic field, with $I_e = 10$ mA, and $E_e = 11$ GeV. We have integrated over a horizontal angular acceptance of $\Delta\theta = 10$ mrad, and a vertical acceptance of $\alpha = \pm 1$. The characteristic spectra of SR and spin-light obtained from these numerical intragrations are shown in Fig. 3. The total power radiated, P_γ(long) and the spin dependent difference of power radiated above and below the orbital plane of the electron, ΔP(long) are shown as a function of photon energy in Fig 3 (a). The number of SR photons N_γ(long) and the number of spin-light photons ΔN_γ(long), as function of photon energy are shown in Fig 3 (b). The asymmetry defined as $A = \frac{\Delta N_\gamma(long)}{N_\gamma(long)}$ as a function of photon energy is shown in Fig. 3 (c).

Fig. 3 (c) indicates that one should measure the hard tail of the SR spectrum ($E_\gamma > 500$ keV) and avoid the soft part of the spectrum where the asymmetry is low and changes rapidly with energy. Although the asymmetry is small $\sim 10^{-4}$ the photon flux is high, even at the hard tail of the spectrum, allowing a rapid determination of the asymmetry, with 1% statistical uncertainty

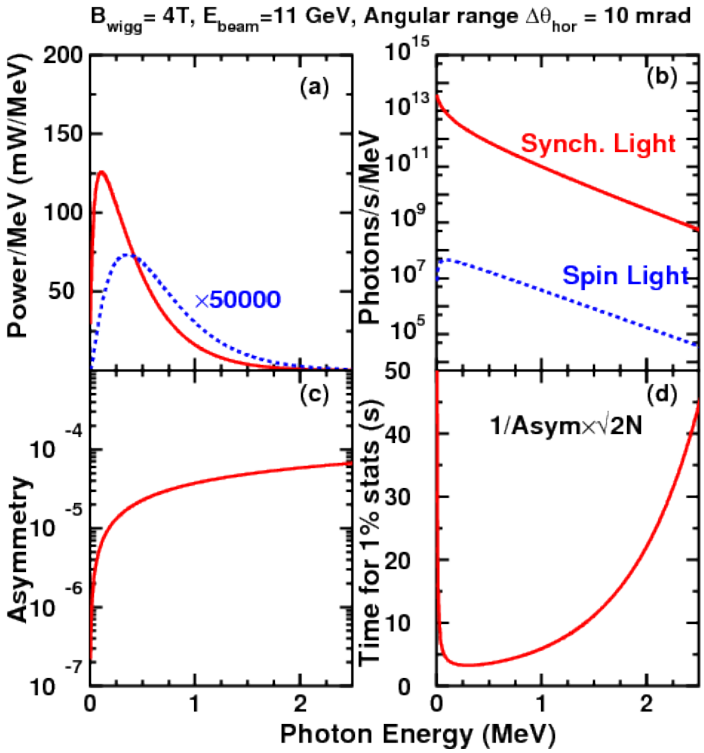

Figure 3: (a) The total SR power radiated, per MeV (solid), and the spin dependent difference in power radiated, per MeV (dashed), above and below the orbital plane, for 11 GeV, longitudinally polarized electrons in a 4 T magnetic field and 10 mA current, 10% detector efficiency and 1% collimation. (b) The total number of SR photons per MeV and the number of "spin-light" photons per MeV, and (c) the asymmetry $\frac{\Delta N}{N}$ as a function of photon energy. (d) The time for 1% statistical uncertainty, in seconds.

within few tens of seconds ($\frac{\delta A}{A} = \frac{1}{A\sqrt{2N}}$) as shown in Fig 3 (d). The energy dependence of the asymmetry for $E_e = 4 - 20$ GeV and the magnetic field dependence of the asymmetry for $B_{wigg} = 2 - 5$ T are shown in Fig 4(a) and Fig 4(b) respectively. These figures demonstrate that a spin-light based polarimetry is a very promising technique at intermediate energies and can be used to monitor the polarization of $4 - 20$ GeV electrons in very rapid measurement cycles, with high statistical precision.

Although the size of the asymmetry increases with increasing electron beam energy it should be noted that the total power of SR, increases as the fourth power of the electron beam energy, and increases linearly with beam current. Moreover, the vertical size of the SR spot decreases with increasing electron beam energy as shown in Fig. 1 (bottom). These factors impose practical limitations on the highest electron beam energies and the highest currents below which a spin-light polarimeter would be feasible. We estimate that it is best suited for the 4 - 20 GeV energy range for currents less than $\sim$ 10 mA.

5 Spin-Light Polarimeter: A Conceptual Design

The two basic components of a spin-light based polarimeter are the source of SR and the X-ray detector which can measure the spatial asymmetry.

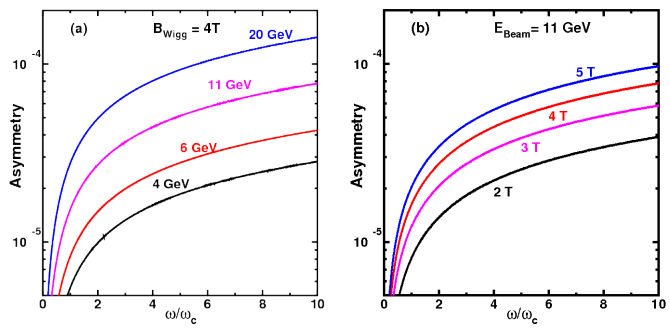

Figure 4: (a) The spin dependent asymmetry as a function of ratio of photon energy to the critical photon energy, for electron beam energy, $E_{beam} = 4 - 20$ GeV. (b) The spin dependent asymmetry for magnetic field, $B_{wigg} = 2 - 5$ Tesla.

5.1 The SR Source - Wiggler

A three pole wiggler magnet with a magnetic field that has uniform magnitude but reversed direction at each pole and a short-long-short pole arrangement is well suited as a source of SR. The three poles must be symmetric about the center such that the line integral of the magnetic field in the direction of the motion of the electron, z, must be zero (i.e. $\int B(z)dz = 0$), ensuring that it does not affect the electron beam transport and its spin direction (beyond the wiggler). The field being of opposite polarity at the 3 poles, flips the sign of the spin dependent spatial asymmetry from any two adjacent poles and hence when measured simultaneously it can help reduce systematic uncertainties arising from the vertical motion of the beam.

The intensity and the asymmetry both increase with increasing field strength, while the pole length decreases with increasing field strength. Therefore a field strength of 4 T is a judicious choice for the wiggler field. A 10 mrad bend can be achieved with a pole length of 10 cm. Thus the total magnet length is 40 cm, and the spacing between the poles is optimized for ease of extraction and detection of the SR beam. A separation of 1 m between the poles allows for collimators to be placed that can separate the SR beams spots from the different poles. The small pole length ensures that the effect of spin-flip inducing SR and the fluctuation of the SR power are negligible ($< 0.1\%$).

Wiggler magnets are regularly used at light sources around the world such as the Advanced Photon Source (APS) at Argonne National Lab and Spring8 in Japan. Some of these magnets are well suited for a spin-light polarimeter [26].

5.1.1 Effect of the wiggler on the electron beam

A non-invasive polarimeter is highly desirable and hence we must study the effect of fluctuations related to the quantum nature of SR produced by the wiggler. The effect of SR on the electron beam were carefully studied for the recirculating arcs [29], and the same methods can be used to calculate the influence of the wiggler on critical beam parameters. As described in Ref. [28] and [29], the distribution of energies lost by individual electrons in bending through some angle θ is given by a convolution of the distribution of the number of photons emitted and the distribution of energies of those photons. The number of photons emitted by a particular electron per radian bend will be distributed according to Poisson statistics about a mean value given by [28], $n = \frac{5}{2\sqrt{3}}\frac{\gamma}{137} = 20.62E$, where n is the mean number of photons per radian bend, and E is the beam energy in GeV. The average energy of the photons emitted is $E_c = \hbar\omega_c = \frac{3}{2}\frac{\hbar c\gamma^3}{R}$ [28]. Therefore the mean energy fluctuation is given by $\Delta E = \sqrt{n}E_c$. It is interesting to note that the energy fluctuation depends

only on the electron beam energy and the bend radius of the wiggler. A beam of 11 GeV electrons in a 4T wiggler with a 10 m bend radius and a bend angle of 10 mrad, gives $n \sim 2$ and $E_c = 199$ keV. Therefore $\Delta E/E \sim 2.5{\times}10^{-5}$, which is comparable to the fluctuations due to the recirculating arcs of the JLab accelerator [29].

The SR power spectrum usually peaks at angles of $\pm 1/\gamma$ with respect to the electron direction. However, if an electron emits on the average two photons in a magnet, the angular distribution of the momentum kick received by each electron is peaked in the direction of the electron's motion. The magnitude of the transverse kicks generated by the emission of a photon with energy E_c in the direction $\theta_\gamma = 1/\gamma$ with respect to the electron direction is given by [28], $\Delta\theta_e = \frac{E_\gamma \sin\theta_\gamma}{E_e} = 11.3 \times 10^{-9} \frac{E_e(GeV)}{R(m)}$. The r.m.s. kick from the emission of n photons is given by $\sqrt{n}\Delta\theta_e$. Thus for a 11 GeV beam bend by 10 mrad the r.m.s. kick is $\sim 1.5 \times 10^{-8}$ rad, which is negligible.

Thus the wiggler magnet would have negligible influence on the electron beam and a spin-light polarimeter can be used for non-invasive monitoring of the beam polarization.

5.1.2 Influence of the wiggler bend direction

The wiggler bend direction was chosen to be beam-left for the conceptual design (see for example Figs. 9 & 10). Since the bend direction is transverse to the asymmetry direction one does not expect any systematic influence due to the choice of the bend direction. However, the design includes two symmetric pairs of ionization chambers placed on either side of the beam, and since the bend is small (10 mrad), it should be possible to build symmetric pairs of collimators and slits on both sides of the beam. With such a setup the independence of the spin-light asymmetry with respect to the wiggler bend direction can be directly verified during calibration and commissioning of the device. For the stability of operation, changes in bend direction during regular operation is not desirable.

5.2 The X-ray Detector - Ionization Chamber

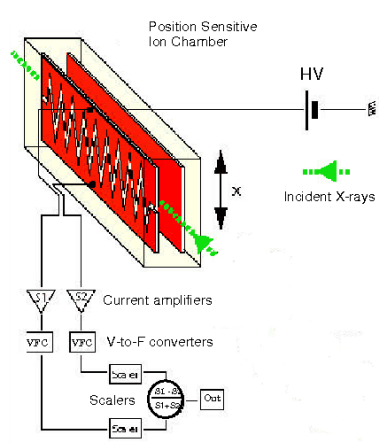

Figure 5: A position sensitive ionization chamber developed at the APS and SPring-8 with a resolution of 5μm when operated at photon flux of $5.0{\times}10^{12}$ 8 keV photons/sec. [27] Note that the image shown here would constitute just one half of a differential ionization chamber required for spin-light polarimetry.

The detector used to measure the spatial asymmetry must be sensitive to X-rays in the range of about 500 keV to 2.5 MeV and must be able to pick out a small asymmetry from a large spin independent background, it must be radiation hard, have low noise and be able to withstand high rates of $\sim 10^{12}$ photons/sec. Ionization chambers (IC) are well known for their high rate capability when operated as an integrating detector (i.e. in current mode), low electronic noise and radiation hardness. Argon/Xenon is an attractive candidate for use as an ionization medium, its high atomic number (18/54) and density (when compressed) gives it a high stopping power for hard X-rays and low energy gamma [30]. Over the last two decades, room temperature, high

pressure (> 50 atm, 0.55 g/cc) xenon (HPXe) ionization chambers have been developed with high detection efficiency in the 50 keV - 2.0 MeV range [23, 24, 25].

Another recent development, is the split collector ionization chamber that have turned the IC into a position sensitive device. Position sensitive ionization chambers are designed to have the collector plate split into two sections in a zig-zag/backgammon pattern such that each half operates as an independent ionization chamber. A prototype of such a chamber has been shown in Fig. 5. These chambers were developed at the APS at ANL and at the SPring-8 light source in Japan. They are used to measure the vertical position of X-ray beams and have been shown to have a resolution of 5 μm [27]. These chambers also have very low dark currents in the ~pA range and have been operated at photon flux of 5.0×10^{12} photons/sec. They work by measuring the difference in counts between the two halves of the chamber, i.e. they are differential ionization chambers (DIC). A position sensitive DIC operated in current mode can be used to measure the spatial asymmetry of the SR generated by longitudinally polarized electrons.

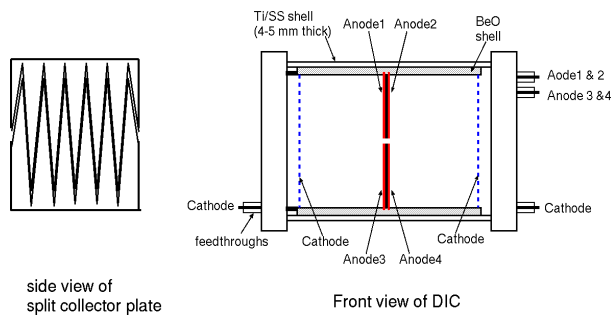

Figure 6: (left) A schematic of the split anode plate. (right) The dual differential ionization chamber for spin-light polarimetry.

A dual, 1 atm. Ar/Xe differential ionization chamber would be ideal for a relative polarimeter. A schematic for such an IC is shown in Fig. 6. The chamber would consist of Ti or stainless steel windows thick enough to cut down the low energy X-rays (< 50 keV). A pair of split central anode plates (separated by a thin insulator) would be placed between the cathodes. The anode plates would be split in a backgammon pattern. The current measured on each half of the anode plates is amplified with a differential current amplifier.

A magnified view of the synchrotron radiation from two adjacent poles of the wiggler magnet incident on a dual DIC is shown in Fig. 7. The left panel of the figure shows the beam's view of the dual DIC. The collimated radiation is shown as oval blobs with the up-down asymmetry represented by the gray shading of the blob (the collimation scheme needed to achieve this is discussed in the next section). The right panel shows an isometric view of the electrodes in the DIC, without showing the incident radiation. The collimated SR beam from two adjacent poles will be incident on opposite sides of the anodes in the dual DIC. The spin-light spatial asymmetry (above and below the orbital plane) will have opposite sign in each half of the DIC because the magnetic field direction of the adjacent poles of the wiggler are opposite. On the other hand any spatial asymmetry due to vertical motion of the beam will have the same sign in the two halves of the dual DIC and hence should cancel to first order. Thus the dual DIC is essential to ensure that the spin-light polarimeter is insensitive to vertical beam motion.

5.2.1 The Signal from the DICs

If we denote $N_{SR}^{L(R)}$ as the number of SR photons on the left(right) of the anode plates, $N_{spin}^{L(R)}$ as the number of spin-light photons, and $\Delta N_z^{L(R)}$ as the difference in number of photons introduce by the vertical beam motion, then the contribution to the measured current from the top left part of the dual DIC will be (see Fig. 7):

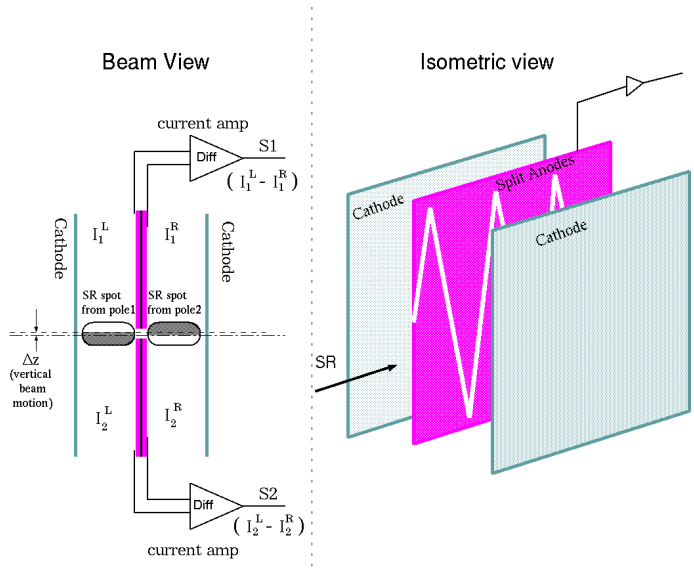

Figure 7: A schematic of the collimated beams of synchrotron radiation from 2 adjacent poles of the wiggler magnet incident on the differential ionization chambers. The figure on the left is a beam's view of the electrodes of the DIC. The collimated radiation is shown as oval blobs, while the figure on the right is an isometric view of the electrodes, without showing the incident radiation.

$$I_1^L \propto N_{SR}^L + N_{spin}^L + \Delta N_z^L,$$

similarly the current contribution from the top right of the dual DIC is:

$$I_1^R \propto N_{SR}^R - N_{spin}^R + \Delta N_z^R.$$

From the simulation studies we estimate that after collimation the size of these currents will be on the order of ~ 10 nA.

Note the change in the sign of the contribution from spin light photons because they are generated from adjacent poles of the wiggler while the contribution from vertical beam motion has the same sign. For the bottom left and right parts of the dual DIC we get;

$$I_2^L \propto N_{SR}^L - N_{spin}^L - \Delta N_z^L,$$

and

$$I_2^R \propto N_{SR}^R + N_{spin}^R - \Delta N_z^R.$$

Thus, the signal from the top and bottom halves of the DIC, $S1$, and $S2$ as shown in Fig. 7, can be written as,

$$\begin{aligned} S1 &\propto (N_{SR}^L + N_{spin}^L + \Delta N_z^L) - (N_{SR}^R - N_{spin}^R + \Delta N_z^R) \\ &= 2N_{spin}, \end{aligned} \tag{9}$$

and

$$\begin{aligned} S2 &\propto (N_{SR}^L - N_{spin}^L - \Delta N_z^L) - (N_{SR}^R + N_{spin}^R - \Delta N_z^R) \\ &= -2N_{spin}. \end{aligned} \tag{10}$$

Hence $S1 - S2 \propto 4N_{spin} \propto 4P_e$, and the vertical motion related asymmetry cancels to first order as does the corrections due to transverse polarization. However, it should be noted that the signals $S1+$

$S2$ is proportional to the transverse polarization of the electron beam, as described in Sec. 4. This possibility of measuring both the longitudinal and transverse asymmetries in the same setup, provides further capability for reducing systematic uncertainties and makes the spin-light polarimeter a versatile tool.

The number of photons absorbed in the ionization chamber can be calculated by multiplying the SR spectrum with the absorption function $A(\lambda) = 1 - e^{-\mu(\lambda)\cdot t}$, where t is the length of the chamber, λ is the photon wavelength and μ is the absorption coefficient which is obtained from NIST database [31]. The number of photons absorbed in a 50 cm long chamber with 1 atm Xe, is shown in Fig. 8(left). Also shown in the absorption weighted (or detector response weighted) asymmetry (right).

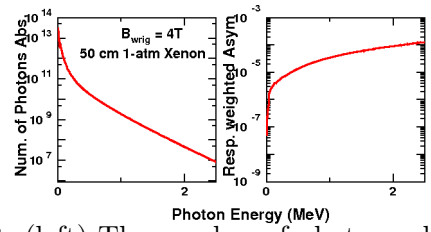

Figure 8: (left) The number of photons absorbed in a 1-atm, 50 cm long Xe chamber. (right) The detector response weighted asymmetry.

5.3 Collimation

The spacing between the wiggler poles was chosen to be 1 m to allow adequate room for the placement of collimators that would separate the SR beams from each pole. The flight path from the wiggler to the detector is selected to be 10 m, which implies that the SR spot size due to each of the wiggler poles will fan out over a horizontal length of $\sim$ 10 cm. The vertical width of the SR spot is only $\sim$ 1 mm. With appropriate placement of collimators on the wiggler pole entrance and exit faces, it is possible to separate the SR beam spot from the four different wiggler poles. The magnet system will wiggle the beam by 10 mrad in the horizontal plane such that each pole of the wiggler magnet produces a fan of synchrotron radiation in the horizontal plane as shown in the top view of the magnets (Fig 9).

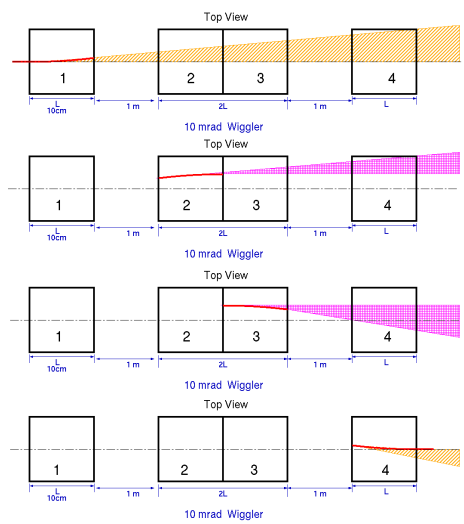

Figure 9: A schematic of the fan of synchrotron radiation produced as the electron beam traverses through each of the 4 poles of the wiggler magnet. The top view of the magnets has been shown. The two hatch-styles are used to indicate that the poles 1 and 4 have opposite polarity compared to poles 2 and 3 and therefore the sign of the asymmetry for the SR fans of the two hatch-styles are opposite.

For longitudinally polarized electrons this fan of synchrotron radiation will have an up-down asymmetry in the vertical direction (due to spin-light). A series of collimators placed at the front and back faces of each pole of the wiggler magnet and at the center of the central pole of the wiggler will be used to select small angular ranges from the entire fan of synchrotron radiation as shown in the top view of the magnets in Fig 10. This collimation scheme enables separation of the synchrotron radiation from each pole of the wiggler magnet. Such a separation is necessary because the up-down asymmetry

of the synchrotron radiation has opposite sign for each pole of the wiggler. Each of the collimated beams of synchrotron radiation will be separated by a few cm when they are projected into two symmetric dual DICs located at a distance of 10 m from the wiggler magnet.

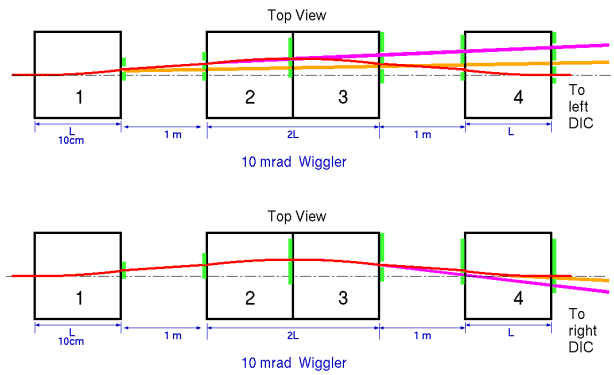

Figure 10: A schematic for the slits and collimators used to select small angular range of the fan of synchrotron radiation. The synchrotron beams from poles 1 and 2 will be incident on the dual DIC placed on the beam left and the beams from poles 3 and 4 are incident on the dual DIC placed on the beam right.

5.4 The Complete Polarimeter

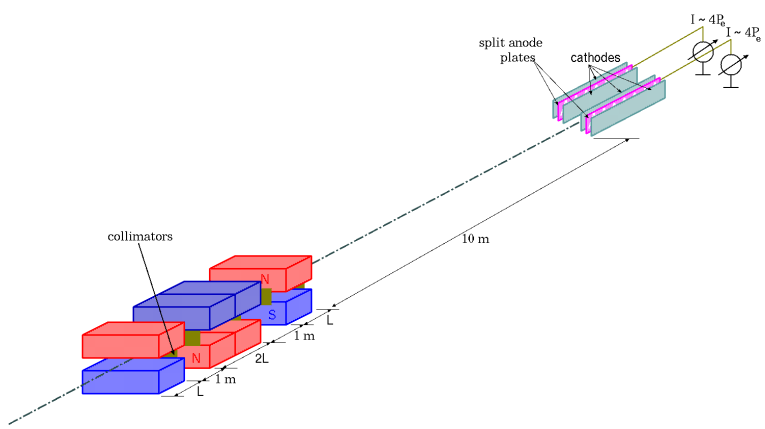

Figure 11: A schematic for a differential spin-light polarimeter (not to scale).

A 3D view of the complete spin-light polarimeter is shown in Fig 11. Each pole of the wiggler magnet is separated by a distance of 1 m and the two dual differential ionization chambers are placed 10 m from the last pole of wiggler magnet. The vertical backgammon split on the central anodes makes the DIC position sensitive in the vertical direction and hence the signal from the DIC is sensitive to the up-down asymmetry for each of the collimated beams of synchrotron radiation. The second dual DIC is necessary to provide an independent measurement of the up-down asymmetry and help reduced systematic uncertainties. The main parameters of this conceptual design are tabulated in Table 2.

Table 2: Parameters of the SR polarimeter at 11 GeV

	Beam & Magnet	
E_e, current	(GeV), (mA),	11.0, 10
$B_{wiggler}$	(T)	4.0
Pole (total) length	(m)	0.1 (0.4)
Separation between poles	(m)	1.0
bend angle	(mrad)	10
vertical opening angle	(mrad)	0.05
Flight path to detector	(m)	10
	SR and detector	
N_γ/s	(Hz)	5.8×10^{13}
ΔN_{Spin}/s	(Hz)	1.8×10^{9}
Detector medium	(1 atm Xe, cm)	50
N_{abs}/s	(Hz)	3.1×10^{12}
$\Delta N_{fluctuation}$/s	(Hz)	7.6×10^{6}
Typical current in DIC	nA	~ 100
vertical beam spot after 10m flight	(mm)	1.0

5.5 Systematic Instrumental Uncertainties

Some of the major sources of systematic uncertainties for a spin-light polarimeter include the background asymmetries from processes such as Bremsstrahlung and false asymmetry due to vertical beam motion, differences in chamber efficiency and magnetic field non-uniformity between adjacent poles of the wiggler. The measured experimental asymmetry from a spin light polarimeter can be written as $A_{expt} = A_{raw}(1+B/S) - A_B B/S + A_F$, where S and B are the signal and background, A_B is the background asymmetry and A_F is the false asymmetry due to factors such as vertical beam motion, differences in the chamber efficiency and differences in the field strength between adjacent poles. The main advantage of operating the ionization chambers as differential detectors is that the false asymmetries will cancel to first order. In addition the visible portion of the synchrotron light can be used to align the detectors and help control systematic uncertainties. The 3-pole design ensures that the vertical beam motion related false asymmetry also cancels to first order. However, the size of the background must be small compared to the signal. In order to address this issue, a full Geant4 [9] simulation of a proto-type spin-light polarimeter was built. The simulation was also used to study the effects of the asymmetry associated with the background. In all of these studies we have assumed that the electron beam satisfies the JLab criteria of **"parity quality"** beam (used by all parity violating experiments at JLab). Under these conditions the helicity correlated beam motion is controlled at the *nm* level and the helicity correlated changes in beam energy are controlled to better than 1 ppb.

In addition to the built-in synchrotron radiation physics available in Geant4, we have implemented a spin-light generator using a parametrized model of spin-light at the nominal running conditions (11 GeV beam, 4T magnetic field and 10 mrad bend angle). Using this generator we were able to reproduce the expected photon energy spectrum and the expected asymmetry as shown in Fig. 12.

The exact position and width of the slits/collimators on the front and back faces of the wiggler

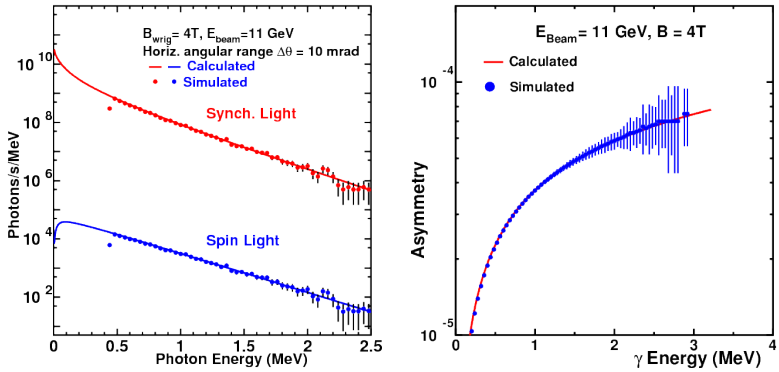

Figure 12: The simulated photon spectrum and asymmetry compared to the calculated spectra for the nominal running conditions.

magnets were optimized iteratively to obtain the best separation between the SR photons originating from the different poles of the magnets. Currently, we are using slits only to illuminate the beam right split ionization chamber. A 3 mm sheet of lead shielding is also applied in front of the ion chamber.

The ionization generated from the photons incident on the ion-chamber is integrated to obtain the signal from the chamber and this signal was used to study several of the systematic uncertainties, such as the effect of background radiation, the position/alignment of the collimators and the alignment of the ion chambers, on the asymmetry signal. The results of these studies have been tabulated in Table 3.

The simulated data show that the background from non-SR radiation is $\sim 1.6\%$ and most of the background is at energies below 0.5 MeV. If the background related dilution can be determined to $\sim 1\%$ the systematic uncertainty due of background radiation will be $\sim 0.5\%$. Moreover, in the proposed setup the background can be determined by measuring the difference in the signal from the chambers with the wiggler magnets turned on and off during calibration and commissioning of the device and at some relatively long interval during regular operations (these background measurements would be invasive in nature).

The same Geant4 simulation was also used to determine the contribution to the systematic uncertainty due to the uncertainty in the exact position and width of the slits and collimators that are placed on the front and back faces of the poles of the wiggler magnets. These collimators are used to separate the SR photons originating from the various poles. Thus, any uncertainty in the position and width of the collimators can give rise to a false asymmetry due to mixing of spin-light and SR photons from different poles. The simulation demonstrates that a position/width uncertainty of 100 μm would lead to a uncertainty of $< 0.2\%$.

We have also simulated the effects of the finite beam size on the up-down asymmetry. The simulations were performed for a beam with a Gaussian distribution of width, σ= 100 μm. The effects of the fringe fields at the tapered edges of the wiggler poles has also been studied using a Poisson Fish [32] model of the magnetic field. Although the absolute photon flux was reduced due the fringe fields the effect on the asymmetry was found to be minimal.

We have studied the effects of beam halos on the spin-light asymmetry. The restrictive collimation scheme discussed in section 5.3 ensures that the contribution from beam halo is very limited. For a ratio of peak to halo of $\sim 10^8$ the dilution to the spin-light asymmetry is several orders of magnitude smaller than the spin-light asymmetry. Thus, for a tightly controlled beam, halos should

not pose a serious challenge.

Table 3: Systematic instrumental uncertainties for a relative polarimeter at $E_{beam} = 11$ GeV.

Source	Uncertainty	$\frac{\delta A}{A}$
Dark current	$\sim$ pA	$< 0.01\%$
Intensity fluctuations	$\Delta N \times 10^{-3}$	<0.1 %
Beam energy	1.0×10^{-3}	< 0.05 %
Density of chamber gas,	relative difference	$<0.01\%$
Slit width	100 μm	<0.2 %
Background related dilutions	known to 0.5% for B/S $\sim$ 0.02	0.5 %
Other dilutions	cancel to first order	$< 0.1\%$
Halo contributions	10^{-8}	< 0.1 %
Total		0.6 %

Most of the systematic uncertainties listed in Table 3 are independent of the electron beam energy in the 4 - 20 GeV range, however, because of the decrease in the SR spot size with increasing electron beam energy the uncertainty due the slit width scales inversely with beam energy.

The proposed device is best used as a relative polarimeter, however, it can be used as an absolute device if the lower and upper bounds of the energy sensitivity of the DIC is determined accurately. The absolute value of the spin light asymmetry depends on the absolute value of the energy window over which the DIC signals are integrated. It is especially sensitive to the lower bound because of the rapid change in the SR intensity and the spin-light asymmetry as a function of decreasing photon energy. For an absolute measurement the lower bound of the integration window would be the dominant source of systematic uncertainty. Excellent energy resolutions have been demonstrated for HPXe ionization chambers [23, 24, 25]. With such high resolution ionization chambers one should be able to determine the response function and the lower bound of energy sensitivity of the chamber to better than 2%. Using a lower bound of 0.5 MeV, the Geant4 based simulation indicate that a variation of $\pm$ 10 keV in the lower bound results in a 2.5% change in the calculated asymmetry. Thus, a spin-light polarimeter would only be capable of $\sim$ 2.5% absolute polarization measurement.

A table of estimated systematic uncertainties is shown in Table 3. We estimate the systematic instrumental uncertainties of a relative polarimeter to be $< 1\%$.

6 Plan of Work

We propose to construct a split plane differential ionization chamber as a prototype of the X-ray detector to be used in a spin-light polarimeter. The prototype differential ionization chamber will be tested using the existing chicane magnets of the Hall-A Compton polarimeter and a 11 GeV longitudinally polarized electron beam to measure the spatial asymmetry in SR from longitudinally polarized electrons. We will also explore testing the prototype differential ionization chamber at other multi-GeV polarized electrons beam facilities (e.g. Novosibirsk). Such a measurement would be the first demonstration of the spin dependence of SR from longitudinally polarized electrons. A possible test setup using the Hall-A chicane magnets is shown in Fig. 13.

In parallel the William and Mary group will develop the complete simulations and the CCD

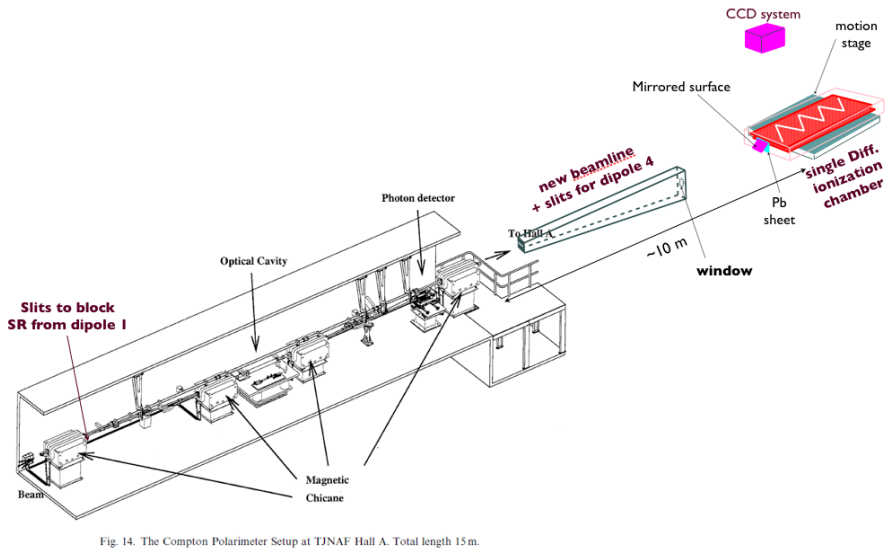

Figure 13: Test setup using the JLab Hall-A Compton chicane magnets.

based optical alignment system which will use the visible portion of the synchrotron radiation to help align the detector and monitor helicity correlated beam motion.

The ANL group has extensive experience with complex detector systems and large installation experiments. They will help with conducting the initial tests of the differential ionization chamber at the APS. They can also help procure surplus wiggler magnets from the APS for the full proto type.

The UVa group has extensive experience with the JLab Hall-A Compton polarimeter and their expertise will be invaluable during the testing of the differential ionization chambers in the Hall-A Compton beamline.

The Stony Brook and Mainz groups, both have extensive polarimetry experience at BNL and MAMI respectively.

The eRHIC design team at BNL, led by Dr. Vladimir Litvinenko and the EIC Task Force at BNL as well as members of the Center for Advanced Studies of Accelerators (CASA) at JLab will be consulted throughout this project and will aid in the design process.

The JLab group had extensive experience with the Hall-C Moller and Compton polarimeters and their expertise will be invaluable during the testing of the differential ionization chambers in the Hall-A Compton beamline.

6.1 Projected Time-line

6.1.1 Year 1

The PI and post-doc Mitra Shabestari from the MSU group will work on the simulation, design and construction of the split-plane differential ionization chamber. Graduate student Valerie Gray from the William and Mary group will also work on this project to design and build the CCD based alignment system. The Mainz group has extensive polarimetry experience and will provide engineering assistance during the design phase of the project.

1. Simulation and Design
The existing Geant simulation will be expanded to incorporate the split-plane in the ionization

chamber. The geometry of the split-plane will be studied in these simulations to help select the best geometry to maximize the position resolution and stability. This work will be performed by the W&M group and the UVa group.
A field map of the Hall-A Compton chicane magnets will be included in the existing Geant simulation of the Synchrotron radiation and spin-light radiation and a full simulation will be carried out. This will help determine the expected signal and ideal location for the detector. This work will be performed by the W&M group and the UVa group.

2. Hardware
Ionization chambers and power supplies will be procured. Current amplifiers and other readout electronics will be procured and tested. This will be carried out by the MSU.
A DAQ system will be setup to test the ionization chamber using radiological sources. This work will be performed by the MSU group.

3. Deliverables
Final design of the split-plane geometry.
Optimized running conditions and detector location.
Tested DAQ setup.

6.1.2 Year 2

The design, construction and initial testing of the differential ionization chamber will be completed in the first two years of the project. The initial tests will be conducted at X-ray sources such at the Advanced Photon Source and the ANL group will help accomplish this task. The W&M group will put together the CCD based alignment and beam motion monitoring system during this period.
1. Simulation and Design
The Geant simulation will be expanded to include the CCD system for the detection of the visible portion of the synchrotron radiation. This simulation will help design the CCD alignment system. This work will be performed at W&M and the UVa group. Engineering assistance with the design of the split-plane chamber will be provided by the University of Mainz
2. Hardware
Build the split-plane for the ion chamber based on results of simulation from year 1.
Assemble split plane ion chamber along with all readout electronics and DAQ developed during year 1. Perform tests of the split-plane ion chamber in the lab using radiological sources and with a X-ray source such as the APS. These tasks will be performed at MSU and ANL.
Build CCD alignment and beam motion monitoring system.
3. Deliverables
A well tested split-plane ion chamber and CCD based alignment system ready for testing in the Hall-A Compton chicane magnets or at any multi-GeV polarized electron source which has access to a chicane/bending magnet.

6.1.3 Year 3

The testing of the prototype chamber in the Hall-A Compton beamline will be completed over the second and third period. Co-PI Dr. Kent Paschke and his group had worked on both the Hall-A and Hall-C Compton polarimeters and they will help carry out the testing of the differential ionization chambers in the Hall-A Compton beamline. During the third years the complete set of prototype differential ionization chambers (four) will be designed based on the tests of the prototype detector. Design and engineering assistance will be provide by University of Mainz group.

During this period, we will begin the process of identifying an existing 4 Tesla prototype wiggler magnets for the spin-light polarimeter. One of the co-PIs Dr. Paul Reimer (Argonne National Lab), will help identify such a wiggler magnet. Wiggler magnets are routinely built at light sources such as the APS at ANL and Spring8 in Japan. Some of these magnets are well suited for a spin-light polarimeter. [26]. We expect to begin the process of identifying, procuring and adapting an appropriate wiggler magnets from the APS.

The beamline vacuum elements and collimators which will help test the prototype chamber in an electron beamline will be constructed in consultation with the members of Center for Advanced Studies of Accelerators (CASA) at JLab. Dr. Arne Freyberger and Dr. Jay Benesch from CASA will collaborate on the design of the beam line elements of the spin-light polarimeter. Engineering assistance will be provide by University of Mainz group.

We will also explore alternative test sites such as the storage ring in Novosibirsk. Co-PI Dr. Abhay Deshpande will help in identifying a suitable test site and organize the effort to test the prototype polarimeter.

1. Simulation and Design
dual split-plane ionization chamber for the full proto type polarimeter. Verify optimized split plane for dual chamber.
Design and implement prototype wiggler magnet in the Geant simulation of the Synchrotron radiation and spin-light radiation. This will help optimize the wiggler design and determine the ideal location for the detector. The same simulation will also help in the design of

Complete simulation and design of a full prototype polarimeter with dual ion chamber, and final design of wiggler magnet. The simulations will also help design the collimators needed and help determine the optical location of the collimators.

2. Hardware
Test the prototype split-plane chamber developed over year 1 and 2 using the JLab Hall-A Compton chicane magnets.
Identify a wiggler magnet for prototype polarimeter based on simulations of year 2.
Design dual ionization chamber based on simulations of year 2.
Build beamline vacuum elements for prototype chamber including slits and collimators.

3. Deliverables
A prototype split-plane ionization chamber tested with polarized electron beam.
Complete design for detectors and vacuum systems for a full prototype spin-light polarimeter that is ready to be build and tested.

Summary
The project timeline is summarized in Table 7.4.

Table 4: Project Timeline

Activity	Year 1	Year 2	Year 3
Design and build prototype DIC	√	√	
Test prototype DIC at the APS		√	
Design and build slits and collimators			√
Test DIC in Hall A Compton beamline (or equivalent)			√
Design CCD based alignment system	√	√	
Build CCD system		√	
Design wiggler magnet			√
Identify suitable wiggler magnet at the APS			√

7 Budget

7.1 Salaries

Funds are requested to support half a post-doc at MSU for all three years. Funds are also requested for half a graduate student at William and Mary for all 3 years. Matching funds are available for the post-doc salary and the graduate student salary. Fringe and overhead is included for both post-doc and graduate student salaries. The post-doc salary is set at $42,000 and the graduate student stipend is set at $20,000 per annum.

7.2 Equipment

During the first two periods a prototype split plane ionization chamber will be built. These will be based on commercially available chambers with a custom made collector plate. The chambers will be long and thin, 30 cm long with an electrode gap of 2.0 cm. The cost of the ion chambers is based on quotes from FMB Oxford. These chambers would then be modified by incorporating a custom electrode with a backgammon split. Several different periods and overlap lengths will be tried. The cost for the split electrodes is based on communication with I. Kuzmenko of the CMS-CAT at the APS. The price for the electronics to read out the ion chambers is based on quotes from FMB-Oxford. The price for power supplies are based on quotes for several different power supplies such as Iseg and Ortec.

The gas handling system for the ion chambers will be very similar to the system built for the GEM detector by the BoNuS collaboration at JLab. The P.I. is part of the collaboration and the price for the gas handing system is based on the P.I.s involvement in the building of the BoNuS detector.

Following the testing of the prototype DIC is the Hall-A Compton beamline, the dual split electrode DICs will be built for the polarimeter. These will have to be custom chambers adapted form the FMB-Oxford chambers. The price for these chambers is based on the price for similar size chambers from FMB-Oxford.

The associated readout electronics for the dual chambers include current amplifiers, V-to-F

converters and scalers. They also include additional power supplies for the dual chambers. The price for these are based on quotes from FMB-Oxford, Iseg and Ortec

The price for the custom beamline vacuum elements which will help mount the detectors is based on quotes from MDC vacuum. They also include slits and collimators. The price for the slits and collimators are based on quotes from FMB-Oxford who specialize in building slits and other detector mounting elements for synchrotron light sources.

The CCD based alignment system will consist of a remotely controllable multi-axis motion stage, associated motor controllers and driver. The price for these items is based on several quotes from motion stage manufacturers such as Dover Motion and IKO. The cost of CCD system, and readout is based on quotes from Thorlabs for a 1280×1024 resolution, 0.5" wide CCD camera with USB based readout. The price for the optics is based on quotes from Thorlabs for lenses, mirrors and mounts.

Equipment	Yr 1	Yr 2	Yr3	Total cost
prototype DIC	10000			10000
Split plane electrodes	5000			5000
Electronics for DIC(2 channels)				
current amps		8000		8000
High voltage power supplies		5000		5000
V-to-Fs and scalers		9000		9000
VME crate		10000		10000
Single board computer		7000		7000
Gas Handling system		5000		5000
Custom beamline vacuum			10000	10000
elements				
slits and collimators			8000	8000
CCD alignment system				
motion stage, controller and driver (1)	8000			8000
high resolution CCD imager	4500			4500
and fast readout (2)				
light transport optics (2)	2500			2500
Total Equipment Cost	30000	43000	18000	91000

Table 5: Equipment cost breakup

7.3 Travel

Funds are requested in each of the three years of the grant to cover domestic travel related to traveling to collaboration meetings and travel to JLab during the later years for testing of ion chambers in the beamline. Travel expenses include overhead charges.

7.4 Total

The year by year breakdown of the budget along with the total request of $292000, is shown in table 7.4.

Item	Year 1	Year 2	Year 3	Total
0.5 Post-doc (MSU)	\$40k	\$40k	\$40k	\$120k
0.5 Grad student (W&M)	\$17k	\$17k	\$ 17k	\$51k
Equipment	\$30k	\$43k	\$18k	\$97k
Travel	\$10k	\$10k	\$10k	\$30k
Total	\$97k	\$110k	\$85k	\$292k

References

[1] P. Mohanmurthy and D. Dutta, to appear in IEEE Tran. in Nucl. Sci.; arxiv:1309.6711.

[2] V. Ptitsyn, private communication.

[3] K. Watanabe *et al.*, Proceedings of the 1993 Particle Accelerator Conference Vol. **5**, 3845 (1993).

[4] A. Daoud *et al.* Procedia Engineering **2**, 1487 (2010).

[5] D. Boer *et al.*, arxiv:1108.1713

[6] M. Hauger *et al.*, Nucl. Inst. Meth. **A462**, 382 (2001).

[7] To be reported for the polarization measured during the QWeak experiment at JLab, Hall-C.

[8] P. C. Rowson, D. Su, and S. Willocq, Ann. Rev. Nucl. Part. Sci. **51**, 345 (2001); M. Woods, SLAC-PUB-7319 (1996).

[9] J. Allison *et al.*, Nucl. Inst. and Meth. **A506**, 250 (2003); J. Allison *et al.*, IEEE Trans. in Nucl. Science **53**, 270 (2006).

[10] D. D. Ivanenko, I. Pomeranchuk, Ya Zh. Eksp. Teor. Fiz. **16**, 370 (1946); J. Schwinger, Phys. Rev. **75**, 1912 (1947).

[11] G. A. Schott, Ann. Phys. **24**, 635 (1907); A. A. Sokolov and I. M. Ternov, Zh. Eksp. Theor. Fiz. **31**, 373 (1956), Sov. Phys. JETP **4**, 396 (1957).

[12] F. R. Elder, R. V. Langmuir and H. C. Pollock, Phys. Rev. **74**, 52 (1948).

[13] M. Yu Ado and P. A. Cherenkov, Sov. Phys. Dokl. **1**, 517 (1957).

[14] F. A. Korolev, E. .N. Akimov, E. N. Markov, and O. F. Kulikov Sov. Phys. Dokl. **1**, 568 (1957).

[15] P. Joos, Phys. Rev. Lett. **4**, 558 (1960).

[16] A. A. Sokolov, N. P. Klepikov and I. M. Ternov, JETF **23**, 632 (1952).

[17] A. A. Sokolov, and I. .M. Ternov, JETF **25**, 698 (1953).

[18] A. A. Sokolov and I. .M. Ternov, *Synchrotron Radiation*, Pergamon Press, New York (1968); A. A. Sokolov and I. .M. Ternov, *Radiation from Relativistic Electrons*, A.I.P. Translation Series, New York (1986).

[19] I. M. Ternov, Physics - Uspekhi **38**, 409 (1995).

[20] V. A. Bordovitsyn, Ph. D. Thesis, Moscow (1983); I. M. Ternov and V. A. Bordovitsyn, Vestn. Mosk. Univ. Ser. Fiz. Astr. **24**, 69 (1983); V. A. Bordovitsyn and V. V. Telushkin, Nucl. Inst. and Meth. **B266**, 3708 (2008).

[21] S. A. Belomesthnykh *et al.*, Nucl. Inst. and Meth. **227**, 173 (1984).

[22] J. Le Duff, P. C. Marin, J. L. Manson, and M. Sommev, Orsay - Rapport Technique, 4-73 (1973).

[23] V. V. Dmitrenko *et al.*, Sov. Phys.-tech. Phys. **28**, 1440 (1983); A. E. Bolotnikov *et al.*, Sov. Phys.-Tech. Phys. **33**, 449 (1988);

[24] C. Levin *et al.*, Nucl. Inst. and Meth. **A332**, 206 (1993).

[25] G. Tepper and J. Losee, Nucl. Inst. and Meth. **A356**, 339 (1995).

[26] E. Nakamura *et al.*, J. of Elec. Spec. and Rel. Phen. **80**, 421 (1996); D. E. Baynham, P. T. M. Clee, and D. J. Thompson, Nucl. Instr. and Meth., **152**, 31 (1978)

[27] K. Sato, J. of Synchrotron Rad., **8**, 378 (2001); T. Gog, D. M. Casa and I. Kuzmenko, CMC-CAT technical report.

[28] M. Sands, SLAC Technical note, SLAC-121 (1970).

[29] B. Norum, CEBAF Technical note, TN-0019 (1985).

[30] A. E. Bolotnikov and B. Ramsey, Nucl. Inst. and Meth. **A396**, 360 (1997).

[31] http://www.nist.gov/physlab/data/xraycoef/index.cfm

[32] http://library.lanl.gov/cgi-bin/getfile?00415886.pdf